Interfacial structure of a mixed dipolar liquid in contact with a charged solid surface

Sanjib Senapati and Amalendu Chandra

Citation: The Journal of Chemical Physics **112**, 10467 (2000); doi: 10.1063/1.481681
View online: http://dx.doi.org/10.1063/1.481681
View Table of Contents: http://scitation.aip.org/content/aip/journal/jcp/112/23?ver=pdfcov
Published by the AIP Publishing

Interfacial structure of a mixed dipolar liquid in contact with a charged solid surface

Sanjib Senapati and Amalendu Chandra[a)]
Department of Chemistry, Indian Institute of Technology, Kanpur, 208016, India

(Received 27 December 1999; accepted 23 March 2000)

We develop a nonlinear theory for the calculation of interfacial structural properties of a dipolar mixture in contact with a charged solid surface. Both the molecular sizes and the dipole moments of various species can be unequal. Explicit numerical results are obtained for the interfacial structure of a binary dipolar liquid in contact with a charged surface of varying surface charge density. The dipole moments of the two species are also varied. The density profiles of both the species are found to be highly inhomogeneous and oscillatory near the solid surface. The more polar species is found to exhibit a positive electrostriction at the surface with an increasing surface electrostatic field. An opposite behavior is observed for the less polar species. The polarization profiles reveal pronounced orientational order of the solvent molecules of both the species near the charged surface. The contact polarizations of the more polar and the less polar species show, respectively, a more than linear and a less than linear increase with increasing surface charge density. The predictions of the present theory for a given set of parameter values are compared with the results of Monte Carlo simulation of the same system and a good agreement is found for the inhomogneous density and polarization profiles of both the species. © *2000 American Institute of Physics.* [S0021-9606(00)51123-4]

I. INTRODUCTION

In recent years, a considerable amount of work has been done concerning the structure of pure dipolar liquids near solid surfaces. Theoretical,[1–17] computer simulation,[18–27] and experimental studies[28–32] have generated significant information about the spatial and orientational arrangement of dipolar molecules in the vicinity of both charged and uncharged solid surfaces. These studies have shown that the structure of a dipolar liquid near a solid surface is highly inhomogeneous and oscillatory revealing layering at molecular level. The orientation of solvent molecules depend critically on the surface charge density. Nonlinear phenomena like the electrostriction and dielectric saturation have been found to be rather significant for dipolar liquids near highly charged surfaces.[16]

However, in contrast to the effort that pure solvents have received, relatively little attention has been focused on the structure of mixed dipolar liquids at solid–liquid interfaces. In fact, we are aware of only one simulation study on this problem[21] and, to the best of our knowledge, no analytical theory has yet been developed to predict the spatial and orientational structure of a dipolar mixture in contact with a charged or an uncharged solid surface. Therefore, there remain a number of unanswered questions regarding such interfacial systems. In particular, the phenomenon of selective adsorption, which is absent in pure solvents, may play a crucial role in determining the spatial and orientational structure of mixed dipolar liquids near solid surfaces. This selective adsorption can originate from unequal molecular size and/or unequal polarity of different components of a solvent mixture.

Our purpose in the present paper is to present a theoretical study of the solid–liquid interfaces involving mixed dipolar liquids. We develop a nonlinear theory for the calculation of interfacial structure of a dipolar mixture in contact with a charged solid surface. The theory is based on a combined approach of the weighted density and the perturbative approximations for the isotropic and anisotropic parts of the solvent densities. Both the molecular sizes and the dipole moments of different components can be unequal. Explicit numerical results are obtained for the interfacial structure of a binary dipolar liquid in contact with a charged surface of varying surface charge density. The dipole moments of the two species are also varied. The density profiles of both the species are found to be highly inhomogeneous and oscillatory near the solid surface. The density of the more polar species at the surface is found to increase with an increasing surface electrostatic field. An opposite behavior is observed for the less polar species. This is a nonlinear effect and a manifestation of the selective adsorption of the more polar species against the other one at the charged surface. The extent of electrostriction is also found to depend on the molecular size. The solvent polarization profiles reveal pronounced orientational order of the solvent molecules of both the species near the charged surface. With increasing surface charge density, the contact polarizations of the more polar and the less polar species show, respectively, a higher and a smaller increase than that predicted by the linearized theory. Thus, the solvent polarizations are found to obey a nonlinear dependence on the surface electrostatic field.

We have also carried out a Monte Carlo (MC) simulation of a binary dipolar liquid confined between two uniformly charged solid surfaces. The separation between the two walls is taken to be sufficiently large so that solvation zones at the two surfaces do not overlap and a bulk region of

a)Electronic mail: amalen@iitk.ac.in

homogeneous density for both the species are found in the middle region of the simulation system. The purpose of carrying out the simulation was to obtain essentially exact results for the spatial and orientational structure of a dipolar mixture near a charged surface so that the accuracy of the present theory could be verified. The predictions of the present theory for a given set of parameter values are compared with the results of Monte Carlo simulation of the same system and a good agreement is found for the inhomogeneous density and polarization profiles of both the species in the interfacial region.

The organization of the rest of the paper is as follows. In Sec. II, we present the theory and the numerical results are discussed in Sec. III. The details of Monte Carlo simulation are described in Sec. IV. Our conclusions are summarized in Sec. V.

II. THEORY

We consider an n-component dipolar mixture consisting of nonpolarizable dipolar molecules that are confined between two uniformly charged solid surfaces. The solvent molecules are modeled as dipolar hard spheres, where the diameter and dipole moment of molecules of different species can be different. The dipolar molecules also interact with the two solid surfaces. The total configurational energy of the mixture can be expressed in the form

$$U=\frac{1}{2}\sum_{\alpha=1}^{n}\sum_{\beta=1}^{n}\sum_{i=1}^{N_\alpha}\sum_{j=1}^{N_\beta}u_{\rm hs}^{\alpha\beta}(r_{ij}) -\frac{1}{2}\sum_{\alpha=1}^{n}\sum_{i=1}^{N_\alpha}\mu_\alpha^i\cdot E_{\mu;\alpha}^i+\sum_{\alpha=1}^{n}U_{w;\alpha}, \tag{1}$$

where N_α is the number of molecules of species α, r_{ij} is the distance between molecule i of species α and molecule j of species β, $u_{\rm hs}^{\alpha\beta}(r_{ij})$ is the hard sphere interaction potential that is equal to ∞ for $r_{ij}<(\sigma_\alpha+\sigma_\beta)/2$ and zero otherwise, where σ_α is the diameter of a solvent molecule of species α. μ_α^i is the dipole moment vector (of magnitude μ_α) of particle i of species α and $E_{\mu;\alpha}^i$ is the electric field at molecule i of species α due to all other dipoles in the mixture. The third term in Eq. (1) arises from the interaction of solvent molecules with the two solid surfaces. We assume that the walls are located at positions z' and z'' along the z axis and x and y axes are parallel to the solid surfaces. For this geometry, the wall–solvent interaction potential can be described as a function of the z coordinate of particle $i(z_i)$ and its orientation (Ω_i) and $U_{w;\alpha}$ can be written as

$$U_{w;\alpha}=\sum_{i=1}^{N_\alpha}u_{w;\alpha}^i(z_i,\Omega_i), \tag{2}$$

with

$$u_{w;\alpha}^i(z_i,\Omega_i)=u'_{w;\alpha}(z_i,\Omega_i)+u''_{w;\alpha}(z_i,\Omega_i), \tag{3}$$

where u' and u'' represent the interaction of particle i of species α with the walls located at $z=z'$ and $z=z''$, respectively. Both u' and u'' include a short range hard sphere–hard wall interaction and a long range electrostatic interaction. Thus, $u'_{w;\alpha}(z_i,\Omega_i)$ can be written as

$$u'_{w;\alpha}(z_i,\Omega_i)=u_{w;\alpha}^{hw}(|z_i-z'|)-E'(z_i)\cdot\mu_\alpha^i, \tag{4}$$

where $u_{w;\alpha}^{hw}(|z_i-z'|)$ is infinity for $|z_i-z'|<\sigma_\alpha/2$ and zero otherwise and $E'(z_i)$ is the electric field produced at z_i by the surface charges of the wall located at z'. In the present calculations, the wall located at z' is assumed to have a positive charge density (σ_c) and the one at z'' is assumed to have a negative charge density of equal magnitude and $z''>z'$. This generates a uniform electric field of magnitude $E=4\pi\sigma_c$ across the system along the positive z direction.

We denote $\rho_\alpha(\mathbf{r},\Omega)$ as the position and orientation dependent number density of species α of the mixture. In density functional theory (DFT), the grand potential of this system at fixed temperature, volume, external field, and chemical potential can be exactly expressed as a functional of the inhomogeneous density distribution,

$$\bar{\Omega}[\rho_\alpha(\mathbf{r},\Omega)]=F[\rho_\alpha(\mathbf{r},\Omega)]+\sum_{\alpha=1}^{n}\int dr\,d\Omega\,\rho_\alpha(\mathbf{r},\Omega) \times[u_{w;\alpha}(\mathbf{r},\Omega)-\bar{\mu}_\alpha], \tag{5}$$

where $u_{w;\alpha}(\mathbf{r},\Omega)$ is the interaction potential between a molecule of species α and the charged hard wall, as given by Eqs. (3) and (4), $\bar{\mu}_\alpha$ is the chemical potential of species α, and T is the temperature. The intrinsic Helmholtz free energy $F[\rho_\alpha(\mathbf{r},\Omega)]$ is a universal functional of density and consists of two components:

$$F[\rho_\alpha(\mathbf{r},\Omega)]=F^{\rm id}[\rho_\alpha(\mathbf{r},\Omega)]+F^{\rm ex}[\rho_\alpha(\mathbf{r},\Omega)], \tag{6}$$

where the ideal gas free energy functional $F_{\rm id}[\rho_\alpha(\mathbf{r},\Omega)]$ is given by

$$F^{\rm id}[\rho_\alpha(\mathbf{r},\Omega)]=\beta^{*-1}\sum_{\alpha=1}^{n}\int d\mathbf{r}\,d\Omega\,\rho_\alpha(\mathbf{r},\Omega) \times[\ln 4\pi\lambda^3\rho_\alpha(\mathbf{r},\Omega)-1], \tag{7}$$

where $\beta^*=1/k_{\rm B}T$, $k_{\rm B}$ is the Boltzmann constant, and λ is the thermal de Broglie wavelength. The excess free energy $F^{\rm ex}[\rho_\alpha(\mathbf{r},\Omega)]$ includes the contribution from intermolecular interactions and it defines the direct correlation functions of different order through functional derivatives, the most important ones being the first and second-order correlation functions defined by[33]

$$c_\alpha^{(1)}(\mathbf{r},\Omega;[\rho_\alpha(\mathbf{r},\Omega)])=-\beta^*\frac{\delta F^{\rm ex}[\rho_\alpha]}{\delta\rho_\alpha(\mathbf{r},\Omega)}, \tag{8}$$

$$c_{\alpha\beta}^{(2)}(\mathbf{r},\mathbf{r}',\Omega,\Omega')=-\beta^*\frac{\delta^2F^{\rm ex}[\rho_\alpha]}{\delta\rho_\alpha(\mathbf{r},\Omega)\,\delta\rho_\beta(\mathbf{r}',\Omega')}. \tag{9}$$

Minimizing the grand potential of Eq. (5) with respect to density and evaluating the chemical potential for the uniform bulk density of the mixture, one obtains the following expression for the equilibrium density of species α in the presence of the solid wall:

$$\rho_\alpha(\mathbf{r},\Omega)=\frac{\rho_\alpha^{(0)}}{4\pi}\exp[-\beta^*u_{w;\alpha}(\mathbf{r},\Omega) +c_\alpha^{(1)}(\mathbf{r},\Omega;[\rho_\alpha(\mathbf{r},\Omega)])-c_\alpha^{(1)}(\rho_\alpha^{(0)}/4\pi)], \tag{10}$$

where $\rho_\alpha^{(0)}$ is the uniform bulk density of species α of the mixture. The application of the density functional method can now proceed by the search for a self-consistent solution of Eq. (10). The above equation is a formally exact relation, which, in principle, may be solved for $\rho_\alpha(\mathbf{r},\Omega)$ if the functional $c_\alpha^{(1)}$ is known. In practice, however, $c_\alpha^{(1)}$ is generally unknown for inhomogeneous systems and so must be approximated. The simplest approximation of $c_\alpha^{(1)}(\mathbf{r},\Omega;[\rho_\alpha(\mathbf{r},\Omega)])$ of an inhomogeneous system involves a perturbative expansion (to first order) in terms of the density inhomogeneity, which makes use of the second-order direct correlation function of the corresponding homogeneous system, and is given by

$$c_\alpha^{(1)}(\mathbf{r},\Omega;[\rho_\alpha(\mathbf{r},\Omega)])-c_\alpha^{(1)}(\rho^{(0)}/4\pi) = \sum_{\beta=1}^{n}\int d\mathbf{r}'\,d\Omega'\,\tilde{c}_{\alpha\beta}^{(2)}(\mathbf{r}-\mathbf{r}',\Omega,\Omega')\times\left(\rho_\beta(\mathbf{r}',\Omega')-\frac{\rho_\beta^{(0)}}{4\pi}\right), \tag{11}$$

where $\tilde{c}_{\alpha\beta}^{(2)}(\mathbf{r}-\mathbf{r}',\Omega,\Omega')$ is the second-order direct correlation function between species α and β of the homogeneous mixture. The z-dependent first-order correlation function $c_\alpha^{(1)}(z,\Omega)$ can be obtained by integrating Eq. (11) over x and y coordinates. For convenience, we write $\tilde{c}_{\alpha\beta}^{(2)}(\mathbf{r}-\mathbf{r}',\Omega,\Omega')$ in terms of angular functions as follows:

$$\tilde{c}_{\alpha\beta}^{(2)}(\mathbf{r}-\mathbf{r}',\Omega,\Omega') = c_{\alpha\beta}^{000}(|\mathbf{r}-\mathbf{r}'|)+c_{\alpha\beta}^{110}(|\mathbf{r}-\mathbf{r}'|)\phi^{110}(\Omega,\Omega') + c_{\alpha\beta}^{112}(|\mathbf{r}-\mathbf{r}'|)\phi^{112}(\Omega,\Omega',\hat{\gamma}), \tag{12}$$

where the angular functions $\phi^{110}(\Omega,\Omega')=(\hat{\mu}\cdot\hat{\mu}')$ and $\phi^{112}(\Omega,\Omega',\hat{r})=3(\hat{\mu}\cdot\hat{r})(\hat{\mu}'\cdot\hat{r})-(\hat{\mu}\cdot\hat{\mu}')$, $\hat{\mu}$ and $\hat{\mu}'$ are the unit vectors along dipole moments of particles located at $\mathbf{r}$ and $\mathbf{r}'$, and $\hat{r}=(\mathbf{r}-\mathbf{r}')/|\mathbf{r}-\mathbf{r}'|$. In Eq. (12), $c_{\alpha\beta}^{000}(|\mathbf{r}-\mathbf{r}'|)$ represents the isotropic or hard sphere part and the second and third terms represent the anisotropic or dipolar parts of the intra- and interspecies direct correlation functions, whose analytical solutions are available within integral equation theories such as mean spherical approximation (MSA).[34–36]

An alternative to Eq. (11) is to adopt the weighted density approximation (WDA) in which $c_\alpha^{(1)}(\mathbf{r},\Omega;[\rho_\alpha(\mathbf{r},\Omega)])$ for the inhomogeneous density is obtained by evaluating the corresponding expression $\tilde{c}_\alpha^{(1)}$ for the homogeneous fluid at an effective density $\bar{\rho}_\alpha(\mathbf{r},\Omega)$. Thus, we write

$$c_\alpha^{(1)}(\mathbf{r},\Omega;[\rho_\alpha(\mathbf{r},\Omega)])-c_\alpha^{(1)}(\rho_\alpha^{(0)}/4\pi) = \tilde{c}_\alpha^{(1)}[\bar{\rho}_\alpha(\mathbf{r},\Omega)]-\tilde{c}_\alpha^{(1)}(\rho_\alpha^{(0)}/4\pi). \tag{13}$$

Although the perturbative approximation, Eq. (11), is simpler to deal with, WDA has been known to provide a better treatment for the hard sphere correlation contributions.[37–41] Therefore, we decompose the total first-order direct correlation function into two parts: $c_\alpha^{(1)}=c_{\alpha;\mathrm{hs}}^{(1)}+c_{\alpha;\mathrm{ex}}^{(1)}$ where $c_{\alpha;\mathrm{hs}}^{(1)}$ is the isotropic hard sphere contribution to the first-order direct correlation function and $c_{\alpha;\mathrm{ex}}^{(1)}$ represents the remaining anisotropic (or excess) contribution that arises from the explicit dipole–dipole electrostatic interactions and also from the coupling of electrostatic and hard sphere interactions. We adopt a partially nonperturbative approach in which we evaluate the isotropic hard sphere contribution $c_{\alpha;\mathrm{hs}}^{(1)}$ using WDA and the remaining anisotropic part $c_{\alpha;\mathrm{ex}}^{(1)}$ through a perturbative approach by using an equation similar to Eq. (11) but involving only the anisotropic terms of the second-order direct correlation function.

Since the density inhomogeneity is only along the z direction, the expressions for the density of the αth species can now be written in the following form:

$$\rho_\alpha(z,\Omega)=\frac{\rho_{\alpha;\mathrm{hs}}(z)}{4\pi}\exp\Bigg[-\beta^* u_{w;\alpha}(z,\Omega) + \sum_{\beta=1}^{n}\int dx\,dy\,d\mathbf{r}'\,d\Omega' \times[c_{\alpha\beta}^{110}(|\mathbf{r}-\mathbf{r}'|;\rho^{(0)})\phi^{110}(\Omega,\Omega') + c_{\alpha\beta}^{112}(|\mathbf{r}-\mathbf{r}'|;\rho^{(0)})\phi^{112}(\Omega,\Omega',\hat{\gamma}) \times[\rho_\beta(z',\Omega')-\rho_\beta^{(0)}/4\pi]\Bigg], \tag{14}$$

where

$$\rho_{\alpha;\mathrm{hs}}(z)=\rho_\alpha^{(0)}\exp\{c_{\alpha;\mathrm{hs}}^{(1)}(\bar{\rho}_{\alpha;\mathrm{hs}}(z))-\tilde{c}_{\alpha;\mathrm{hs}}^{(1)}(\rho_\alpha^{(0)})\}. \tag{15}$$

Here $\tilde{c}_{\alpha;\mathrm{hs}}^{(1)}(\bar{\rho}_{\alpha;\mathrm{hs}}(z))$ refers to the hard sphere contribution to the first-order correlation function defined through WDA at an effective density $\bar{\rho}_{\alpha;\mathrm{hs}}(z)$ that is obtained as the weighted average $\bar{\rho}_{\alpha;\mathrm{hs}}(z)=\Sigma_{\beta=1}^{n}\int dz'\,\rho_{\alpha;\mathrm{hs}}(z')w_{\alpha\beta}(|z-z'|;\bar{\rho}_{\alpha;\mathrm{hs}}(z))$. The weight function $w_{\alpha\beta}(z-z')$ is calculated by following the prescription of Denton and Ashcroft[38] described later.

We expand the position and orientation dependent solvent density $\rho_\alpha(z,\Omega)$ in the basis set of spherical harmonics as follows:[42,43]

$$\rho_\alpha(z,\Omega)=\sum_{lm} a_{\alpha;lm}(z)Y_{lm}(\Omega), \tag{16}$$

so that the angle-averaged density $\rho_\alpha(z)=\sqrt{4\pi}a_{\alpha;00}(z)$ and the polarization $P_\alpha(z)$ is related to $a_{\alpha;10}(z)$ by the following relation:

$$P_\alpha(z)=\sqrt{\frac{4\pi}{3}}\mu_\alpha a_{\alpha;10}(z). \tag{17}$$

We next substitute Eq. (16) and the explicit forms of the angular functions ϕ^{110} and ϕ^{112} into Eq. (14) and carry out the angular integrations to obtain the following simplified equations for the inhomogeneous solvent density and the polarization for the αth species:

$$a_{\alpha;00}(z)=\frac{\rho_{\alpha;\mathrm{hs}}(z)}{\sqrt{4\pi}}\left(\frac{\sinh\{\beta^*\mu_\alpha E(z)+I_{\alpha;1}(z)+I_{\alpha;2}(z)\}}{\beta^*\mu_\alpha E(z)+I_{\alpha;1}(z)+I_{\alpha;2}(z)}\right), \tag{18a}$$

$$a_{\alpha;10}(z)=\left(\frac{3}{4}\right)^{1/2}\rho_{\alpha;\mathrm{hs}}(z)\times\left(\frac{\cosh\{\beta^*\mu_\alpha E(z)+I_{\alpha;1}(z)+I_{\alpha;2}(z)\}}{\beta^*\mu_\alpha E(z)+I_{\alpha;1}(z)+I_{\alpha;2}(z)}-\frac{\sinh\{\beta^*\mu_\alpha E(z)+I_{\alpha;1}(z)+I_{\alpha;2}(z)\}}{[\beta^*\mu_\alpha E(z)+I_{\alpha;1}(z)+I_{\alpha;2}(z)]^2}\right), \tag{18b}$$

where $I_{\alpha;1}(z)$ and $I_{\alpha;2}(z)$ are given by

$$I_{\alpha;1}(z)=\sum_{\beta=1}^{n}\int dz'\, a_{\beta;10}(z')c_{\alpha\beta}^{110}(z-z'), \tag{19a}$$

and

$$I_{\alpha;2}(z)=\sum_{\beta=1}^{n}\int dx\,dy\,d\mathbf{r}'a_{\beta;10}(z')c_{\alpha\beta}^{112}(|\mathbf{r}-\mathbf{r}'|)\times\left(\frac{3|z-z'|^2}{|\mathbf{r}-\mathbf{r}'|^2}-1\right), \tag{19b}$$

where $c_{\alpha\beta}^{110}(z-z')$ is obtained from $c_{\alpha\beta}^{110}(|\mathbf{r}-\mathbf{r}'|)$ by integrating over x and y coordinates. One can also derive an expression for the quantity $\langle\cos\theta_\alpha\rangle_z$, the average value of $\cos\theta_\alpha$ for a solvent molecule of species α at position z from the surface. The expression of $\langle\cos\theta_\alpha\rangle_z$ is given by

$$\langle\cos\theta_\alpha\rangle_z=\mathcal{L}[\beta^*\mu_\alpha E+I_{\alpha;1}(z)+I_{\alpha;2}(z)], \tag{20}$$

where $\mathcal{L}$ refers to the Langevin function, defined as $\mathcal{L}(x)=\coth(x)-x^{-1}$. The expression for $\langle\cos\theta_\alpha\rangle_z$ in the above equation includes the effects of dielectric saturation in presence of a highly charged surface, since $\langle\cos\theta_\alpha\rangle_z$ in the Langevin form approaches the saturated value of unity at large field strengths. Equations (16)–(20) constitute a set of nonlinear equations for the calculation of the spatial and orientational structure of a mixed dipolar solvent in contact with charged solid surfaces.

In the present work, we have solved the above equations by using MSA solutions for $c_{\alpha\beta}^{110}(|\mathbf{r}-\mathbf{r}'|)$ and $c_{\alpha\beta}^{112}(|\mathbf{r}-\mathbf{r}'|)$ for a binary dipolar mixture. In the MSA, the isotropic part of the two-particle direct correlation function is given by the Percus–Yevick hard sphere correlation function. For a binary mixture of unequal sized hard spheres, the solutions are given by[44,45]

$$c_{\alpha\alpha;\mathrm{hs}}^{000}(|\mathbf{r}-\mathbf{r}'|)=c_{\mathrm{PY}}(|\mathbf{r}-\mathbf{r}'|)=a_\alpha+b_\alpha|\mathbf{r}-\mathbf{r}'|+d'|\mathbf{r}-\mathbf{r}'|^3,\quad \alpha=1,2, \tag{21}$$

for $|\mathbf{r}-\mathbf{r}'|<\sigma_\alpha$ and zero otherwise, while

$$c_{\alpha\beta;\mathrm{hs}}^{000}(|\mathbf{r}-\mathbf{r}'|)=a_\gamma+\Theta(R)[bR^2+4\lambda\, d'R^3+d'R^4]/|\mathbf{r}-\mathbf{r}'|, \tag{22}$$

for $|\mathbf{r}-\mathbf{r}'|<\sigma_{\alpha\beta}$ and zero otherwise. Here Θ is the Heaviside step function, $\lambda=|\sigma_\alpha-\sigma_\beta|/2$, $R=|\mathbf{r}-\mathbf{r}'|-\lambda$, $\sigma_{\alpha\beta}=(\sigma_\alpha+\sigma_\beta)/2$, and the γ component refers to the species of smaller molecular diameter. The coefficients, a_α, b_α, b, and d' depend on the bulk densities of the two components and on the diameter ratio. The analytical expressions of these coefficients are given in the work of Ashcroft and Langreth.[45] The anisotropic terms can be expressed in terms of the Percus–Yevick hard sphere correlation function by the following equations:[36]

$$c_{\alpha\beta}^{110}(r)=2\kappa_{\alpha\beta}[c_{\mathrm{PY}}(r,\rho_1^{+\alpha\beta},\rho_2^{+\alpha\beta})-c_{\mathrm{PY}}(r,\rho_1^{-\alpha\beta},\rho_2^{-\alpha\beta})], \tag{23}$$

$$c_{\alpha\beta}^{112}(r)=c_{\alpha\beta}^{(0)112}(r)-\frac{3}{r^3}\int_0^r dr'\,r'^2c_{\alpha\beta}^{(0)112}(r'), \tag{24}$$

where

$$c_{\alpha\beta}^{(0)112}(r)=\kappa_{\alpha\beta}[2c_{\mathrm{PY}}(r,\rho_1^{+\alpha\beta},\rho_2^{+\alpha\beta})+c_{\mathrm{PY}}(r,\rho_1^{-\alpha\beta},\rho_2^{-\alpha\beta})], \tag{25}$$

and vanishes at $r>(\sigma_\alpha+\sigma_\beta)/2$, where $r=|\mathbf{r}-\mathbf{r}'|$. The modified densities $\rho_m^{+\alpha\beta}$ and $\rho_m^{-\alpha\beta}$ are defined as

$$\rho_m^{+\alpha\beta}=2\frac{\kappa_{\alpha m}\kappa_{m\beta}}{\kappa_{\alpha\beta}}\rho_m, \tag{26a}$$

$$\rho_m^{-\alpha\beta}=-\frac{\kappa_{\alpha m}\kappa_{m\beta}}{\kappa_{\alpha\beta}}\rho_m, \tag{26b}$$

where the index m labels the mth species. The quantities κ_{11}, κ_{12}, and κ_{22} are obtained from the solutions of the following three coupled equations:[36]

$$\frac{4\pi}{3}\beta^*\rho_1\mu_1^2=\Phi_{11}(2\kappa_{11}\rho_1,2\kappa_{12}^2\rho_2/\kappa_{11})-\Phi_{11}(-\kappa_{11}\rho_1,-\kappa_{12}^2\rho_2/\kappa_{11}), \tag{27a}$$

$$\frac{4\pi}{3}\beta^*\rho_1\mu_1\mu_2=\Phi_{12}(2\kappa_{11}\rho_1,2\kappa_{22}\rho_2)-\Phi_{12}(-\kappa_{11}\rho_1,-\kappa_{22}\rho_2), \tag{27b}$$

$$\frac{4\pi}{3}\beta^*\rho_2\mu_2^2=\Phi_{22}(2\kappa_{12}^2\rho_1/\kappa_{22},2\kappa_{22}\rho_2)-\Phi_{22}(-\kappa_{12}^2\rho_1/\kappa_{22},-\kappa_{22}\rho_2), \tag{27c}$$

where

$$\Phi_{\alpha\beta}(\rho_1,\rho_2)=\rho_\alpha\frac{\partial\beta^*\,\mu_\alpha(\rho_1,\rho_2)}{\partial\rho_\beta}, \tag{28}$$

where $\beta^*=1/k_BT$ and $\mu_\alpha(\rho_1,\rho_2)$ is the chemical potential of the αth species in the binary hard sphere mixture whose analytical expression is given in Ref. 36.

We have calculated the weight functions of Eq. (15) by using the prescription of Denton and Ashcroft.[38] In this scheme, the weight functions for a binary hard sphere mixture are specified first by the normalization condition

$$\int d\mathbf{r}\,w_{\alpha\beta}(\mathbf{r})=1,\quad \alpha,\beta=1,2, \tag{29}$$

which ensures that the approximation is exact in the limit of a uniform mixture and, second, by requiring that the first functional derivatives of $\tilde{c}_{\alpha;\mathrm{hs}}^{(1)}$ with respect to the densities

yield the exact two-particle direct correlation functions in the uniform limit. One then obtains the following analytic forms for the weight functions:

$$w_{\alpha\beta}(\mathbf{r}-\mathbf{r}')=\frac{\tilde{c}^{(2)}_{\alpha\beta;\mathrm{hs}}(\mathbf{r}-\mathbf{r}')}{\partial\tilde{c}^{(1)}_{\alpha;\mathrm{hs}}/\partial\rho}. \tag{30}$$

The analytic solutions for the two-particle direct correlation functions of a uniform binary mixture of unequal-sized hard spheres within a Percus–Yevick approximation are given by Eq. (22). These solutions lead to the following simplified expressions for the planar-averaged weight functions $w_{\alpha\beta}(z)$,[38]

$$w_{11}(z)=\frac{\pi}{\partial\tilde{c}^{(1)}_1/\partial\rho}\left(a_1(\sigma_1^2-z^2)+\frac{2}{3}b_1(\sigma_1^3-z^3)+\frac{2}{5}d'(\sigma_1^5-z^5)\right),\quad z<\sigma_1, \tag{31a}$$

$$w_{12}(z)=\frac{\pi}{\partial\tilde{c}^{(1)}_1/\partial\rho}\left(a_1(\sigma_{12}^2-z^2)+\frac{2}{3}b\sigma_1^3+2\,d'\lambda\sigma_1^4+\frac{2}{5}d'\sigma_1^5\right),\quad z<\sigma_{12}, \tag{31b}$$

$$w_{22}(z)=\frac{\pi}{\partial\tilde{c}^{(1)}_2/\partial\rho}\left(a_2(\sigma_2^2-z^2)+\frac{2}{3}b_2(\sigma_2^3-z^3)+\frac{2}{5}d'(\sigma_2^5-z^5)\right),\quad z<\sigma_2. \tag{31c}$$

By integrating the above expressions of the two-particle hard sphere direct correlation functions with respect to **r**, one obtains explicit expressions of the density derivative $\partial\tilde{c}^{(1)}_{\alpha;\mathrm{hs}}/\partial\rho$ for $\alpha=1,2$. The one-particle hard sphere correlation function $\tilde{c}^{(1)}_{\alpha;\mathrm{hs}}$ is then obtained by integrating $\partial\tilde{c}^{(1)}_{\alpha;\mathrm{hs}}/\partial\rho$ over density numerically by following the trapezoidal rule.

We have solved Eqs. (18a) and (18b) iteratively by the standard method of discretization and integration by the trapezoidal rule. In the iteration process, the old profiles of $a_{\alpha;00}(z)$ and $a_{\alpha;10}(z)$ ($\alpha=1,2$) are used on the right-hand side to get the new ones on the left-hand side, and the process is repeated until convergence is reached. To obtain convergence, we have used the known technique of mixing the old solution with the new ones during iteration with the help of a mixing parameter ξ. The value of ξ is taken to be 0.005 and the process required a few thousand iterations before reaching convergence.

III. NUMERICAL RESULTS

The systems studied in this work are specified by the values of the following reduced parameters: the bulk density of species α, $\rho^*_\alpha=\rho_\alpha\sigma^3_\alpha$; the dipole moment of a molecule of species α, $\mu^*_\alpha=\sqrt{\mu^2_\alpha/k_\mathrm{B}T\sigma^3_\alpha}$; the molecular size ratio, $\Gamma=\sigma_2/\sigma_1$; and the electric field produced by the two charged surfaces, $E^*=E\sqrt{\sigma^3_1/k_\mathrm{B}T}$. For all the systems considered in this work, we have chosen $\rho^*_1=0.11$, $\rho^*_2=0.63$, and $\Gamma=1.5$. The dipole moments of the two species are varied, as discussed later. In the numerical calculations, we have used

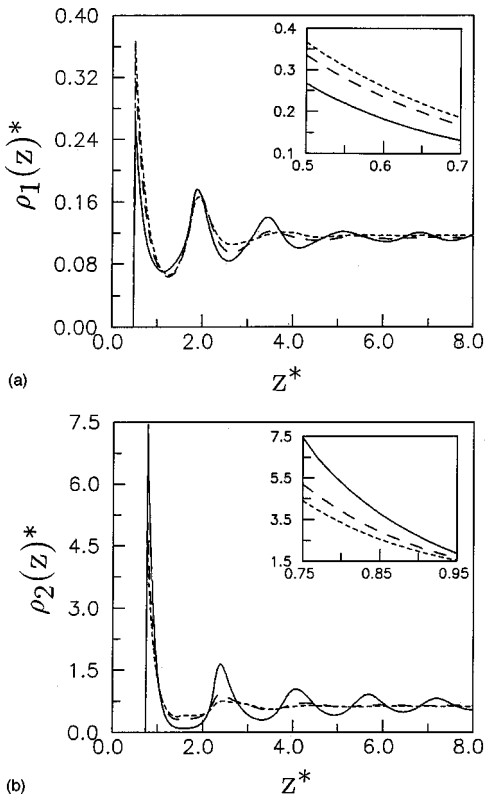

FIG. 1. The variation of the reduced number density of (a) species 1 and (b) species 2 of a binary dipolar solvent in contact with a charged solid surface. The short-dashed, long-dashed, and solid curves are for $E^*=0$, 2, and 4, respectively. The reduced distance $z^*=z/\sigma_1$. Other reduced quantities are specified in the text. The inset shows the solvent densities near the charged surface.

three different values of the electric field: $E^*=0$, 2, and 4. We note that the value of $E^*=4$ corresponds to $E=5.2\times10^9\ \mathrm{V\,m^{-1}}$ and a surface charge density $\sigma_c=0.05\ \mathrm{C\,m^{-2}}$ for $\sigma_1=2.8\ \text{Å}$ and $T=298\ \mathrm{K}$. These values are realizable in practice. For a fully ionized surface, the value of E is about $1.7\times10^{10}\ \mathrm{V\,m^{-1}}$ and the value of σ_c is about $0.3\ \mathrm{C\,m^{-2}}$. In fact, the values of E and σ_c for $E^*=4$ are very close to the ones used in the experiment of Toney *et al.*[29] In the present work, we have discussed the results of the inhomogeneous density and polarization in terms of the reduced quantities: $\rho_\alpha(z)^*=\rho_\alpha(z)\sigma^3_\alpha$ and $P_\alpha(z)^*=P_\alpha(z)\sqrt{\sigma^3_\alpha/k_\mathrm{B}T}$.

In Fig. 1, we have shown the results of the density profiles of the two solvent species near a charged surface for three different values of the surface electric field. The values of the dipole moments are $\mu^*_1=0.65$ and $\mu^*_2=1.29$. The corresponding results of the field dependence of the density changes of both the species in the interfacial region are shown in Fig. 2. It is seen that the density profiles are highly nonuniform near the surface. Also, the density of the first species (less polar) near the surface decreases whereas that of the second species (more polar) increases with an increasing surface electrostatic field. This implies that the charge density of the surfaces attracts the more polar molecules and leads to a stronger physisorption at the charged surface. The opposite effect is observed for the less polar molecules. The increase or decrease of solvent density near a charged surface is a measure of the electrostriction caused by the charge

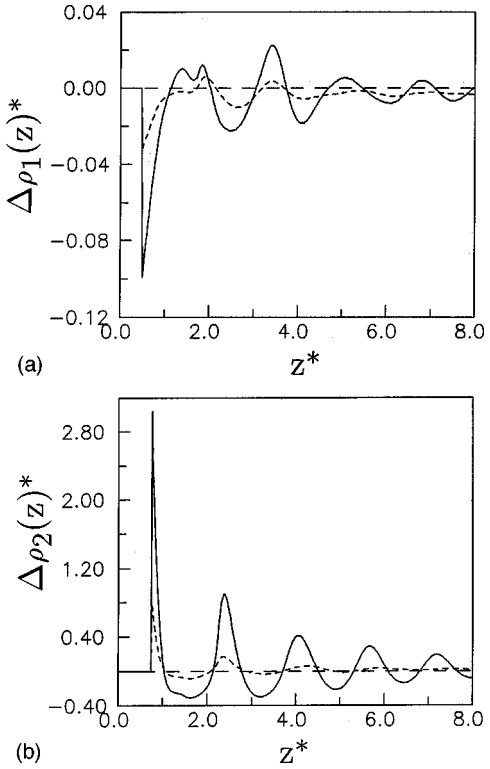

FIG. 2. The variation of the change in reduced number density $\Delta\rho_\alpha(z)^*$ $[=\rho_\alpha(z,E)^*-\rho_\alpha(z,E=0)^*]$ of (a) species 1 and (b) species 2 with the distance from the charged surface. The dashed and the solid curves are for $E^*=2$ and 4, respectively.

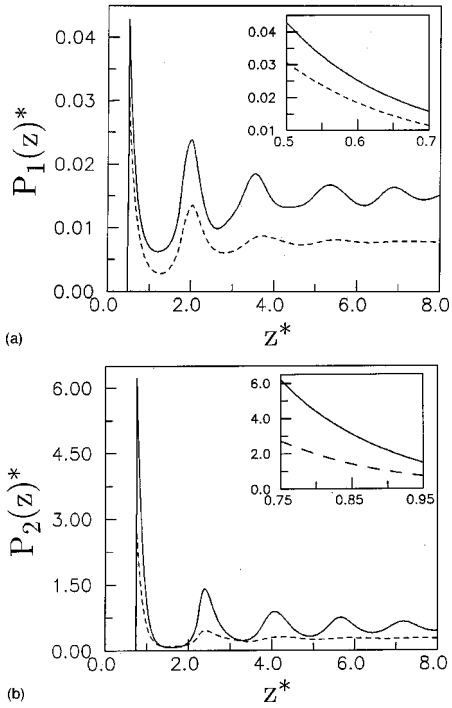

FIG. 3. The variation of reduced polarization of (a) species 1 and (b) species 2 with the distance from the charged surface. The dashed and the solid curves are for $E^*=2$ and 4, respectively. The inset shows the solvent polarization near the charged surface.

density of the surfaces. It is seen that the change of interfacial densities are rather significant for systems of higher surface charge density. This is a nonlinear effect that cannot be obtained in a linearized theory.

The results of the polarization profiles of the two components are shown in Fig. 3. The values of the dipole moments are the same as in Figs. 1–2. The polarizations are found to be most significant near the surface and then they oscillate until bulk values are reached. The range of oscillations increases with increase of the solvent polarity and the surface electric field. Also, the polarization profiles are found to increase with surface charge density in a nonlinear fashion. For example, the predicted values of the contact polarization of component 2 is higher than the corresponding values obtained by linearizing Eq. (14), whereas the polarization profiles of component 1 show an opposite behavior. This nonlinear change of solvent polarization is partly due to the positive and negative electrostriction for species 2 and 1, respectively, near the charged surfaces. Clearly, the electrostriction and polarization effects are coupled with each other. In Fig. 4, we have plotted the quantity $\langle\cos\theta_\alpha\rangle_z$ for two different values of the external electric field E^*. $\langle\cos\theta_\alpha\rangle_z$ describes the average orientation of solvent molecules of species α at a distance z from the charged surface that is located at $z=0$ and it is unity when the molecules are completely oriented along the electric field. The solvent molecules of both the species are found to be more oriented near the surface than in the bulk. Also, the profiles of both $\langle\cos\theta_1\rangle_z$ and $\langle\cos\theta_2\rangle_z$ are seen to oscillate with the distance from the surface, which can be attributed to the competing effects of the surface electric field and the dipole–dipole interactions.

In order to extend the range of our investigation, we have calculated the interfacial density and polarization profiles for a mixture of different dipole moments of the two species. In this system, the species 1 is strongly polar with $\mu_1^*=2.37$ and species 2 is weakly polar with $\mu_2^*=0.35$. The size ratio and other parameter values remain the same as in previous calculations. Thus, in terms of absolute magnitudes, the dipole moments of species 1 and 2 of this system are the same as those of species 2 and 1, respectively, of Figs. 1–4. The density and polarization profiles are obtained for three different values of the surface electrostatic field $E^*=0$, 2, and 4 and the results of the density changes $\Delta\rho_\alpha(z)$ ($\alpha=1,2$) are shown in Fig. 5. It is found that the density of the first species near the surface increases whereas that of the second species decreases with an increasing surface electrostatic field. This again implies that the charge density of the surfaces attracts the more polar molecules and leads to a stronger physisorption at the charged surface compared to that of the weakly polar species. However, the magnitudes of the positive and negative electrostriction observed here are different from those of Fig. 2. This difference may be attributed to the size effect. In Fig. 2, the more polar species also had bigger molecular size, whereas, in Fig. 5, the more polar species is characterized by a smaller molecular size. As expected, the polarization profiles show oscillatory behavior. The polarization of the more polar species is higher than that of the less polar species at the surface although the actual

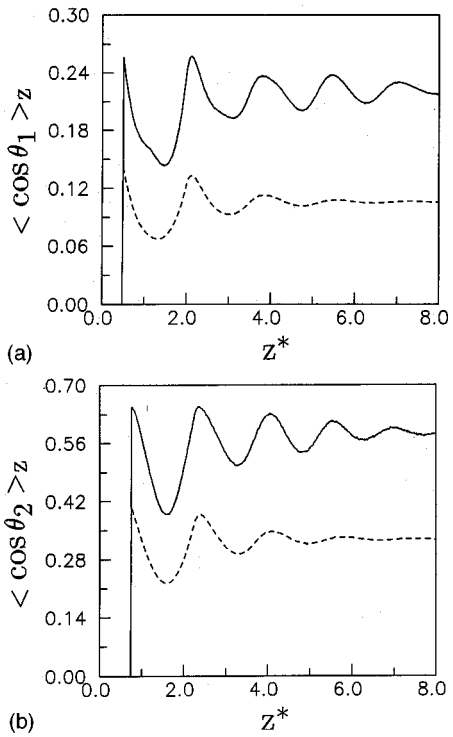

FIG. 4. The variation of $\langle \cos \theta_\alpha \rangle_z$ of (a) species 1 and (b) species 2 with the distance from the charged surface. The dashed and the solid curves are for $E^*=2$ and 4, respectively.

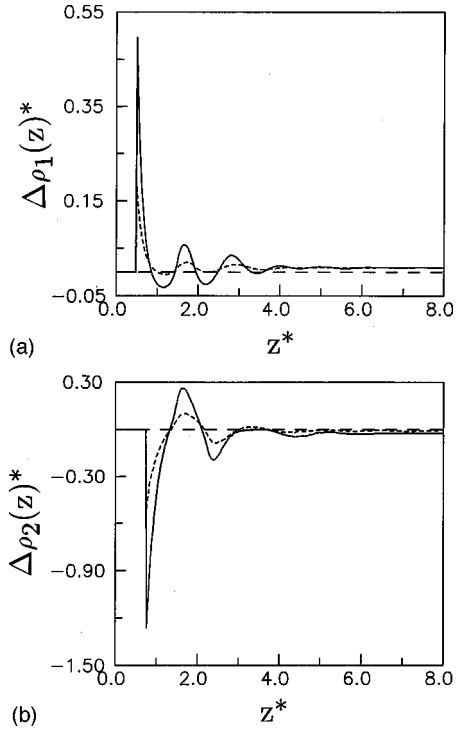

FIG. 5. The variation of the change in reduced number density $\Delta\rho_\alpha(z)^*$ $[=\rho_\alpha(z,E)^*-\rho_\alpha(z,E=0)^*]$ of (a) species 1 and (b) species 2 with the distance from the charged surface. The values of the dipole moments are $\mu_1^*=2.37$ and $\mu_2^*=0.35$. The values of the other parameters are the same as in Fig. 1. The dashed and the solid curves are for $E^*=2$ and 4, respectively.

magnitudes are different from those of Fig. 3, which can again be attributed to the molecular size effect.

IV. MONTE CARLO SIMULATION

We have carried out a Monte Carlo simulation of a binary dipolar liquid confined between two uniformly charged hard walls in order to verify the predictions of the present theory. The dipolar mixture is characterized by the same parameters as were considered in Figs. 1–4. The value of E^* is taken to be 2. The simulation was carried out with a total of 256 molecules (93 of species 1 and 163 of species 2) in a rectangular box with dimension $L\times L\times h$, where h is the separation between the walls and L is the length of the central simulation box in the x and y directions. The walls are located at $z=0$ and $z=10.5\sigma_1$ and the periodic boundary conditions were set at 0 and $9.1\sigma_1$ along the x and y directions. This ensures a bulk region of homogeneous densities $\rho_1^*=0.11$ and $\rho_2^*=0.63$ in the middle region of the simulation system. In the simulation, the long-range dipolar interactions are treated by using the Ewald summation (slab adapted) method.[46] The Ewald parameters employed are the convergence parameter $\alpha/L=6.4$, a reciprocal space cutoff of $15\sigma_1^{-1}$, and $\epsilon'=\infty$, where ϵ' is the dielectric constant of the medium that surrounds the infinite array of periodically replicated systems. The minimum image convention was used for the real space portion of the Ewald sum. In the MC simulation, the system was first equilibrated for 25 000 MC passes and then the simulations were run for another 50 000 MC passes for the calculation of the final averages.

The number densities of the two solvent species are calculated by computing the average number of molecules in slabs of thickness $\Delta z=0.02\sigma_1$. The orientational structure of solvent molecules are calculated by finding the solvent polarization along the field direction (z), which is obtained by calculating the total dipole moment along the z direction in different slabs at various distances from the solid surfaces. In Fig. 6, we have compared the theoretical and simulation results for the number densities of species 1 and 2 at various distances from the charged surfaces. In Fig. 7, we have compared the results for the polarizations of the two components. It is seen that the overall agreement between the theoretical and the simulation results is quite good. Especially, the oscillatory and layered structure of the density and polarization profiles of both the species in the interfacial region is correctly predicted by the present theory.

V. SUMMARY AND CONCLUSIONS

We have presented a nonlinear theory for the calculation of the structure of a mixed dipolar liquid in contact with a charged solid surface by using a density functional approach. Both the molecular sizes and the dipole moments of various species can be unequal. The theory is based on a combined approach of the weighted density approximation for the isotropic part and the perturbative approximation for the anisotropic part of the solvent densities. In the weighted density approximation, the isotropic part of the inhomogeneous density is calculated by evaluating the corresponding isotropic part of the one-particle direct correlation function at an ef-

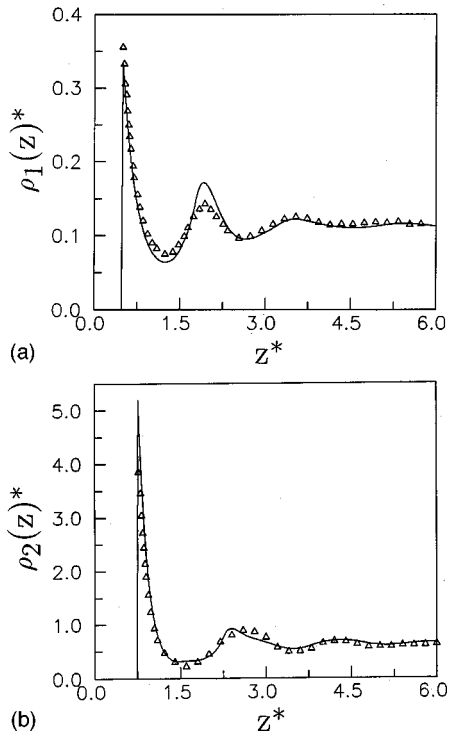

FIG. 6. A comparison of the theoretical and Monte Carlo simulation results of the density profiles of (a) species 1 and (b) species 2 of a dipolar mixture in contact with a charged surface characterized by $E^*=2$. The solid curve represents the results of present theory and the triangles represent the simulation results for the same external field. The values of other parameters are the same as in Fig. 1.

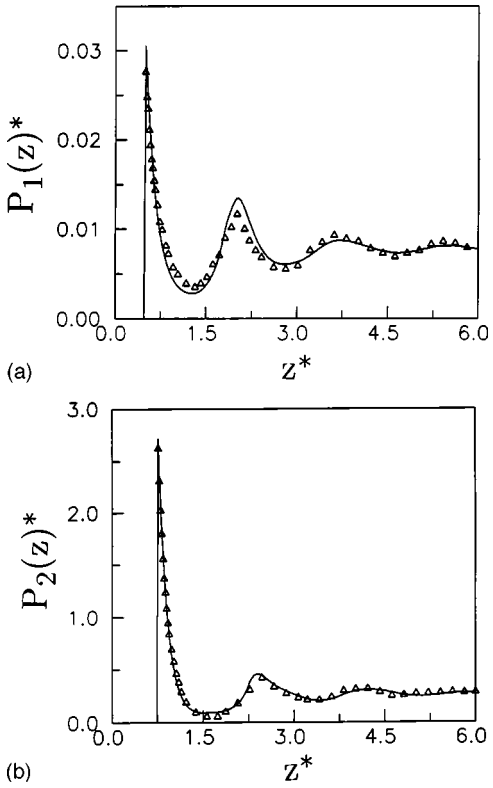

FIG. 7. A comparison of the theoretical and Monte Carlo simulation results of the polarization profiles of (a) species 1 and (b) species 2 of a dipolar mixture in contact with a charged surface. The values of the various parameters are the same as in Fig. 6.

fective density $\bar{\rho}$. In the perturbative approximation, we expand the one-particle direct correlation function of the inhomogeneous system in terms of the density inhomogeneity (to first order) around the corresponding homogeneous system. Thus, the two-particle direct correlation function that appears in Eq. (14) corresponds to the one of the homogeneous system. The motivation for making this approximation is to make use of the analytical solutions of the anisotropic parts of the two-particle intra- and interspecies direct correlation functions that are known for homogeneous dipolar mixtures within theories like MSA.[35,36] We also note that similar perturbative expansion has also been used before for ionic systems[39,40] and also for pure dipolar liquids.[15,16] In the present theory, the interfacial density and polarization profiles depend on the surface–solvent and the solvent–solvent interactions in a nonlinear fashion. The density profiles of both the species are found to be highly inhomogeneous and oscillatory near the surface. The detailed molecular structure of a dipolar species in the interfacial region depends on the bulk density, dipolar strength, and also on the surface electric field. The more polar species is found to exhibit a positive electrostriction at the surface with an increasing surface field. An opposite behavior is observed for the less polar species.

We have also carried out Monte Carlo (MC) simulation of a binary dipolar mixture confined between two uniformly charged surfaces in order to verify the accuracy of the present theory. The results of the simulation are compared with the theoretical predictions for a specified set of parameter values, and a good agreement is found for the inhomogeneous density and polarization profiles of both the species in the interfacial region.

The theory presented in this work is quite general and can be applied to a mixture of any two dipolar liquids, as long as appropriate values of the dipole moments and the molecular diameters are used. Although the basic methodology is known in the literature for pure liquids, here it is extended for the first time to treat dipolar mixtures of unequal size and polarity. The objective has been to obtain the analytical results for a model system and compare the results with the ones of MC simulation. The parameters are chosen to prepare such a model system with different molecular size and polarity and surface electrostatic field. Although we have not chosen the parameter values corresponding to any specific dipolar mixture, we note that the polarity of the two components considered in the numerical calculations does correspond to many real dipolar liquids. For example, the polarity of the weakly dipolar component of the mixture considered in Figs. 1–4 and also in MC simulation roughly corresponds to that of ethyl formate, methyl acetate, ethyl ether, dimethoxyethane, or dimethyl carbonate and the polarity of the more polar component corresponds roughly to that of liquids like 1-butanol, 2-butanol, or 2-methyl-1-propanol, etc. Of course, the parameter values can be changed to represent more polar liquids like acetone, methanol, acetonitrile, or water.

The present theory can be extended in various directions to study the interfacial properties of more complex systems. For example, it would be interesting to study the structure of

electrolyte solutions near charged surfaces when molecularity of both the ions and solvent molecules are considered. It would also be interesting to study the structure of mixed dipolar liquids and ionic solutions near metal surfaces. It would also be worthwhile to formulate an extension of the present theory to dynamical regime. We hope to address these issues in future publications.

ACKNOWLEDGMENTS

We thank Dr. S. K. Ghosh for many enlightening discussions. The financial support of the Council of Scientific and Industrial Research, Government of India, is gratefully acknowledged.

[1] *Fundamentals of Inhomogeneous Fluids*, edited by D. Henderson (Marcel Dekker, New York, 1992).
[2] G. M. Torrie, P. G. Kusalik, and G. N. Patey, J. Chem. Phys. **88**, 7826 (1988); **89**, 3285 (1988).
[3] D. Berard and G. N. Patey, J. Chem. Phys. **95**, 5281 (1991).
[4] D. R. Berard, M. Kinoshita, X. Ye, and G. N. Patey, J. Chem. Phys. **101**, 6271 (1994).
[5] G. Rickayzen and M. J. Grimson, J. Chem. Soc., Faraday Trans. 2 **78**, 893 (1982).
[6] M. Moradi and G. Rickayzen, Mol. Phys. **68**, 903 (1989).
[7] V. Russier, J. Chem. Phys. **90**, 4491 (1989).
[8] P. Frodl and S. Dietrich, Phys. Rev. E **48**, 3741 (1993).
[9] C. E. Woodward and S. Nordholm, Mol. Phys. **60**, 415 (1987); **60**, 441 (1987).
[10] C. E. Woodward and S. Nordholm, J. Phys. Chem. **92**, 497 (1988).
[11] Z. Tang, L. E. Scriven, and H. T. Davis, J. Chem. Phys. **97**, 494 (1992).
[12] V. Russier, M. L. Rosinberg, J. P. Badiali, D. Levesque, and J. J. Weis, J. Chem. Phys. **87**, 5012 (1987).
[13] M. J. Booth, D. Duh, and A. D. J. Haymet, J. Chem. Phys. **101**, 7925 (1994).
[14] R. Akiyama and F. Hirata, J. Chem. Phys. **108**, 4904 (1998).
[15] C. N. Patra and S. K. Ghosh, J. Chem. Phys. **106**, 2752 (1997).
[16] D. Das, S. Senapati, and A. Chandra, J. Chem. Phys. **110**, 8129 (1999); S. Senapati and A. Chandra, Phys. Rev. E **59**, 3140 (1999).
[17] A. Chandra, S. Senapati, and D. Sudha, J. Chem. Phys. **109**, 10 439 (1998).
[18] S. H. Lee, J. C. Rasaiah, and J. B. Hubbard, J. Chem. Phys. **85**, 5232 (1986).
[19] C. Y. Lee, J. A. McCammon, and P. J. Rossky, J. Chem. Phys. **80**, 4448 (1984).
[20] S. Senapati and A. Chandra, J. Chem. Phys. **111**, 1223 (1999); Chem. Phys. **231**, 65 (1998).
[21] S. Senapati and A. Chandra, Chem. Phys. **242**, 353 (1999).
[22] S.-B. Zhu and G. W. Robinson, J. Chem. Phys. **94**, 1403 (1991).
[23] X. Xia and M. Berkowitz, Phys. Rev. Lett. **74**, 3193 (1995).
[24] N. I. Christou, J. S. Whitehouse, D. Nicholson, and N. G. Parsonage, Mol. Phys. **55**, 397 (1985).
[25] J. P. Valleau and A. A. Gardner, J. Chem. Phys. **86**, 4171 (1987).
[26] E. S. Boek, W. J. Briels, J. van Eerden, and D. Feil, J. Chem. Phys. **96**, 7010 (1992).
[27] K. Raghavan, K. Foster, K. Motakabbir, and M. Berkowitz, J. Chem. Phys. **94**, 2110 (1991).
[28] J. N. Israelachvili, *Intermolecular and Surface Forces* (Academic, New York, 1992).
[29] M. F. Toney, J. N. Howard, J. Richer, G. L. Borges, D. G. Wiesler, D. Yee, and L. D. Sorensen, Nature (London) **368**, 444 (1994).
[30] M. F. Toney, J. N. Howard, J. Richer, G. L. Borges, J. G. Gordon, O. R. Melroy, D. G. Wiesler, D. Yee, and L. D. Sorensen, Surf. Sci. **335**, 326 (1995).
[31] J. D. Porter and A. S. Zinn, J. Phys. Chem. **97**, 1190 (1993).
[32] K. Ataka, T. Yotsuyanagi, and M. Osawa, J. Phys. Chem. **100**, 10 664 (1996).
[33] J. P. Hansen and I. R. McDonald, *Theory of Simple Liquids* (Academic, London, 1986).
[34] M. S. Wertheim, J. Chem. Phys. **55**, 4291 (1971).
[35] S. A. Adelman and J. M. Deutch, J. Chem. Phys. **59**, 3971 (1973).
[36] D. Isbister and R. J. Bearman, Mol. Phys. **28**, 1297 (1974).
[37] P. Tarazona, Phys. Rev. A **31**, 2672 (1985); **32**, 3148 (1985).
[38] A. R. Denton and N. W. Ashcroft, Phys. Rev. A **44**, 8242 (1991); **39**, 426 (1989).
[39] Z. Tang, L. Mier-Y-Teran, H. T. Devis, L. E. Scriven, and H. S. White, Mol. Phys. **71**, 369 (1990).
[40] C. N. Patra and S. K. Ghosh, Phys. Rev. E **49**, 2826 (1994); **50**, 5123 (1994).
[41] C. N. Patra, J. Chem. Phys. **111**, 6573 (1999).
[42] B. Bagchi and A. Chandra, Adv. Chem. Phys. **80**, 1 (1991).
[43] C. G. Grey and K. Gubbins, *Theory of Molecular Fluids* (Clarendon, Oxford, 1984).
[44] J. L. Lebowitz, Phys. Rev. **133**, A895 (1964).
[45] N. M. Ashcroft and D. C. Langreth, Phys. Rev. **156**, 685 (1967).
[46] J. Shelley and G. N. Patey, Mol. Phys. **88**, 385 (1996).